Zero-Forcing Beamforming for RIS-Enhanced Secure Transmission

Zhenni Wang, Xiaolan Zhao, Jie Tang, *Senior Member, IEEE*, Nan Zhao, *Senior Member, IEEE*, Daniel K. C. So, *Senior Member, IEEE*, Xiu Yin Zhang, *Fellow, IEEE*, and Kai-Kit Wong, *Fellow, IEEE*

***Abstract*—This article considers a reconfigurable intelligent surface (RIS) enhanced multi-antenna secure transmission system in the presence of both active eavesdroppers (AEves) and passive eavesdroppers (PEves). We propose a zero-forcing (ZF) beamforming strategy that can steer transmit beam to the null space of AEves' channel, while simultaneously enhancing the SNRs for a legitimate user equipment (UE) and PEves without perfect channel state information (CSI). The design goal is to maximize the SNR of UE subject to the transmit power constraint at the BS, SNR limitations on PEves, and reflection constraints at RIS. Due to the complexity of modeling, we first introduce a homogeneous Poisson point process (HPPP) to imitate the distribution of spatially random PEves, which derives a complicated non-convex problem. We then develop an efficient alternating algorithm where the transmit beamforming vector and the reflective beamforming vector are obtained by convex-concave procedure (CCP) and semi-definite relaxation (SDR) technique, respectively. Simulation results validate the performance advantages of the proposed optimized design.**

***Index Terms*—Reconfigurable intelligent surface, physical layer security, beamforming.**

I. Introduction

PHYSICAL layer security (PLS) techniques have been envisioned as a pivotal paradigm for guarding wireless communication systems [1]. Given practical encryption methods operating on the application layer, PLS schemes are considered as an alternative to resist information leakage to eavesdroppers without requiring strong computing power and high-quality hardware implementation [2]. However, traditional PLS schemes such as cooperative relaying schemes [3] incur high hardware costs, while artificial noise (AN) aided beamforming [4] and cooperative jamming [5] are inevitably power-hungry.

To combat security breaches in a more energy-efficient and sustainable way, reconfigurable intelligent surface (RIS) is inspired and introduced into the contemporary secure transmission system [6]. By befittingly tuning the passive reflecting elements of the RIS, the propagation environment can be reconstructed such that the desired signal can bypass the malicious users and target the intended ones. Moreover, the merits of small volume, lightweight, and perfect ductility make RIS easier to be coated on surfaces of skyscrapers in the city.

The main attraction of RIS-aided PLS techniques is the flexibility of simultaneously enhancing or suppressing signal beams to different users [7]. The works in [8] and [9] considered incorporating RIS into the single-user downlink system confronting a single eavesdropper to improve the system secrecy rate by jointly optimizing the transmit covariance at the base station (BS) and phase shift matrix at the RIS. The works in [10] and [11] investigated a RIS-aided secrecy communication system where the transmit beamforming with AN and the reflective beamforming at RIS are jointly designed. The effective AN approach, which can provide the transmitter with additional degree of freedom (DoF), has been confirmed valid especially when the number of eavesdroppers exceeds that of transmit antennas. However, in cases where the BS has a power restriction or a multitude of transmit antennas, the loss outweighs the gain. Moreover, to the best of our knowledge, all the aforementioned works are under the assumption that the perfect channel state information (CSI) of the eavesdroppers is available at the BS, which is unrealistic and incomprehensive in practice. Although passive eavesdroppers (PEves) have been investigated in a few RIS-enhanced PLS works, it is noteworthy that even fewer works focused on the scenario where the confidential message is subject to interception conducted by both passive and active eavesdroppers (AEves).

In the considered RIS-aided downlink MISO communication system, we jointly design the secure beamforming vectors both at the BS and RIS. A homogeneous Poisson point process (HPPP) is implemented to model randomly distributed PEves. Our main contributions are as follows:

- We consider a wiretapping group mingled with multiple AEves and PEves. Unlike prior works, we assume that the locations and the CSI of the PEves remain completely unknown.
- To counter malicious interception, we formulate an SNR maximization problem at the legitimate user and alternatively optimize beamforming vectors under constraints at BS, RIS and eavesdroppers.
- We exploit a novel zero-forcing (ZF) algorithm to design the beamforming vector to lie in the null space of the AEves' channel matrix, then solve the problem following the alternating optimization (AO) procedure.
- Analytical results are provided to show the superiority of the proposed ZF beamforming scheme in achieving SNR targets via RIS.

II. System Model and Problem Formulation

A. RIS-Enhanced Secure Transmission System

As shown in Fig. 1, we construct a RIS-aided downlink secure transmission system in dense urban agglomeration. Suppose an M-antenna BS (Alice) intends to securely deliver confidential data to a legitimate user (Bob) with a single antenna, while numerous obstacles block its way. A RIS (Rose)

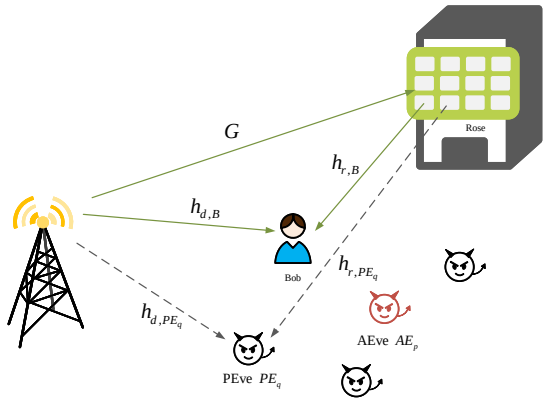

Fig. 1. A RIS-enhanced secure transmission system in urban scenario

with N passive reflecting elements is mounted on the building wall, playing the role of assisting the information transmission from Alice to Bob in the presence of non-colluding eavesdroppers (Eves). Eves set $\mathcal{E} \triangleq \{AE_p, PE_q\}$ encompasses the unauthorized set of N_A AEves and unpredictable number of PEves. It is assumed that Alice knows the CSI of AEves while the CSI of PEves remains totally unknown; thus an HPPP Φ_{PE} with density λ_{PE} has been applied to describe the dynamic geometrical locations of PEves.

The baseband equivalent channels from Alice to Bob, Eve e and Rose are denoted by $\boldsymbol{h}_{d,B} \in \mathbb{C}^{M\times 1}$, $\boldsymbol{h}_{d,e} \in \mathbb{C}^{M\times 1}$ and $\boldsymbol{G} \in \mathbb{C}^{N\times M}$; the channels from Rose to Bob and Eve e are correspondingly denoted as $\boldsymbol{h}_{r,B} \in \mathbb{C}^{N\times 1}$ and $\boldsymbol{h}_{r,e} \in \mathbb{C}^{N\times 1}$. The phase shift matrix of the RIS is defined as $\boldsymbol{\Theta} = \mathrm{diag}\left(\beta_1 e^{j\theta_1}, ..., \beta_N e^{j\theta_N}\right)$, where $\beta_n \in [0,1]$ is the reflection amplitude of the n-th reflecting element of RIS. Moreover, define $\boldsymbol{\nu} = \left[\beta_1 e^{j\theta_1}, ..., \beta_N e^{j\theta_N}\right]^H$ as the reflective beamforming vector, each element of which is required to satisfy $|\nu_n| \leq 1$. All channels are presumed in accordance with quasi-static flat fading distribution.

Let an i.i.d. circularly symmetric complex Gaussian (CSCG) random variable $s(t)$ represents the desirable message for Bob. $\boldsymbol{w} \in \mathbb{C}^{M\times 1}$ is the transmit beamforming vector at Alice who holds a maximum transmit power budget denoted by P_A. The received signals at Bob and Eve e are expressed as

$$y_B(t) = \left(\boldsymbol{h}_{r,B}^H \boldsymbol{\Theta} \boldsymbol{G} + \boldsymbol{h}_{d,B}^H\right) \boldsymbol{w} s(t) + n_B(t), \tag{1}$$

$$y_e(t) = \left(\boldsymbol{h}_{r,e}^H \boldsymbol{\Theta} \boldsymbol{G} + \boldsymbol{h}_{d,e}^H\right) \boldsymbol{w} s(t) + n_e(t), \tag{2}$$

where $n_B(t) \sim \mathcal{CN}\left(0, \sigma_B^2\right)$ and $n_e(t) \sim \mathcal{CN}\left(0, \sigma_e^2\right), \forall e \in \mathcal{E}$ denote the additive white Gaussian noise (AWGN) at Bob and Eve e, accordingly. It can be seen that the received signals consist of signal from both direct and reflective link where Alice-Rose-Bob channel can be considered as replenishment especially when the direct link is very weak. For notational simplicity, the time index is omitted from the remainder of this correspondence. In this single-user multi-eavesdropper secure system, the received SNR at Bob and Eve e can be shown as follows

$$\mathrm{SNR}_B = \frac{\left|\left(\boldsymbol{h}_{r,B}^H \boldsymbol{\Theta} \boldsymbol{G} + \boldsymbol{h}_{d,B}^H\right) \boldsymbol{w}\right|^2}{\sigma_B^2}, \tag{3}$$

$$\mathrm{SNR}_e = \frac{\left|\left(\boldsymbol{h}_{r,e}^H \boldsymbol{\Theta} \boldsymbol{G} + \boldsymbol{h}_{d,e}^H\right) \boldsymbol{w}\right|^2}{\sigma_e^2}. \tag{4}$$

For convenience, we assume $\sigma_B^2 = \sigma_e^2 = \sigma^2$, and $\boldsymbol{h}_B^H = \boldsymbol{h}_{r,B}^H \boldsymbol{\Theta} \boldsymbol{G} + \boldsymbol{h}_{d,B}^H$ and $\boldsymbol{h}_e^H = \boldsymbol{h}_{r,e}^H \boldsymbol{\Theta} \boldsymbol{G} + \boldsymbol{h}_{d,e}^H$ as effective channel vectors from Alice to the receivers. Additionally, the average SNR of PEves should be specifically formulated due to its probabilistic property

$$\begin{aligned} \overline{\mathrm{SNR}}_{PE} &= \mathbb{E}\left[\frac{\boldsymbol{w}^H \boldsymbol{h}_{PE_q} \boldsymbol{h}_{PE_q}^H \boldsymbol{w}}{\sigma^2}\right] \\ &= \frac{\boldsymbol{w}^H \mathbb{E}\left[\boldsymbol{h}_{PE_q} \boldsymbol{h}_{PE_q}^H\right] \boldsymbol{w}}{\sigma^2} = \frac{\boldsymbol{w}^H \overline{\mathbf{H}}_{PE} \boldsymbol{w}}{\sigma^2}, \end{aligned} \tag{5}$$

where $\overline{\mathbf{H}}_{PE} = \mathbb{E}\left[\boldsymbol{h}_{PE_q} \boldsymbol{h}_{PE_q}^H\right]$.

B. SNR Maximization Problem

In this work, we focus on maximizing the received SNR at Bob by jointly optimizing the reflective beamforming vector at Rose as well as the transmit beamforming vector at Alice. In order to guarantee the received SNR at Bob, stipulating Eves' SNR thresholds is necessary. Without any knowledge of PEves' locations, it is rational to take average SNR of PEves into consideration. We choose an appropriate SNR upper bound for PEves and apply a zero-forcing scheme to AEves to avoid information leakage. Accordingly, the coordinated beamforming optimization can be formulated as:

$$\max_{\boldsymbol{w},\boldsymbol{\nu}} \quad \mathrm{SNR}_B \tag{6a}$$

$$\text{s.t.} \quad \overline{\mathrm{SNR}}_{PE} \leq \xi, \tag{6b}$$

$$\mathrm{SNR}_{AE_p} = 0, \tag{6c}$$

$$|\nu_n| \leq 1, \tag{6d}$$

$$\|\boldsymbol{w}\|^2 \leq P_A, \tag{6e}$$

where ξ in (6b) is the SNR upper threshold of PEves, and (6c) enforces the SNR constraint on AEves to be zero by discreetly implementing ZF beamforming design at Alice; (6d) represents the reflection constraint at Rose and P_A in (6e) is the maximum transmit power limit at Alice.

III. RIS-Enhanced Zero-Forcing Beamforming

First of all, we delicately design the transmit beamforming vector and satisfy the constraint (6c). While considering the limited average SNR of PEves, we exploit a zero-forcing scheme to suppress the SNR of AEves to zero. Suppose that a RIS-aided secure transmission system includes one AEve, the designed ZF beamforming vector can be attained by projecting Bob's channel onto the null space of the AEve, which can be written as

$$\boldsymbol{w} = \boldsymbol{\varphi}_{AE_1} \boldsymbol{\varphi}_{AE_1}^H \boldsymbol{h}_B, \tag{7}$$

where $\boldsymbol{\varphi}_{AE_1} \in \mathbb{C}^{M\times(M-1)}$ is a matrix, and its $M-1$ columns form a basis for the null space of the AEve's effective channel vector, such that we obtain

$$\boldsymbol{h}_{AE_1}^H \boldsymbol{\varphi}_{AE_1} = 0, \tag{8}$$

where $\boldsymbol{h}_{AE_1}^H = \boldsymbol{h}_{r,AE_1}^H \boldsymbol{\Theta} \boldsymbol{G} + \boldsymbol{h}_{d,AE_1}^H$. Now, the received signal at AEve can be acquired by

$$y_{AE_1} = \boldsymbol{h}_{AE_1}^H \boldsymbol{\varphi}_{AE_1} \boldsymbol{\varphi}_{AE_1}^H \boldsymbol{h}_B s + n_{AE_1} = n_{AE_1}. \tag{9}$$

Obviously, by steering the transmit beam to the null space of AEve's channel, AEve is unable to overhear tailored messages for Bob. Therefore, after achieving SNR targets of AEves , we now have

$$\begin{aligned} \max_{\boldsymbol{w},\boldsymbol{\nu}} \quad & \mathrm{SNR}_B && (10a)\\ \text{s.t.} \quad & \overline{\mathrm{SNR}}_{PE} \le \xi, && (10b)\\ & |\nu_n| \le 1, && (10c)\\ & \|\boldsymbol{w}\|^2 \le P_A, && (10d) \end{aligned}$$

So far, we have derived an SNR maximization problem marked as problem (10). Owing to the intricate coupling of variable $\boldsymbol{w}$ and $\boldsymbol{\nu}$, problem (10) is non-convex and hence we will leverage on an AO procedure to tackle it in the following parts.

A. Reflective Beamforming Vector Optimization

In this section, we endeavor to tackle problem (10) on the basis of the classic AO structure. Under any fixed transmit beamforming vector $\boldsymbol{w}$ in that problem, we initially introduce an auxiliary variable ρ and optimize the reflective beamforming vector in problem (11) as follows

$$\begin{aligned} \max_{\boldsymbol{\nu},\rho} \quad & \rho && (11a)\\ \text{s.t.} \quad & \frac{\left|\left(\boldsymbol{h}_{r,B}^H \boldsymbol{\Theta} \boldsymbol{G} + \boldsymbol{h}_{d,B}^H\right)\boldsymbol{w}\right|^2}{\sigma^2} \ge \rho, && (11b)\\ & \mathbb{E}\left[\frac{\left|\left(\boldsymbol{h}_{r,PE_q}^H \boldsymbol{\Theta} \boldsymbol{G} + \boldsymbol{h}_{d,PE_q}^H\right)\boldsymbol{w}\right|^2}{\sigma^2}\right] \le \xi, && (11c)\\ & |\nu_n| \le 1. && (11d) \end{aligned}$$

To decouple the optimizing variable $\boldsymbol{\nu}$ out of the equations, we redefine the reflective link from Alice to receivers as $\boldsymbol{h}_{r,B}^H \boldsymbol{\Theta} \boldsymbol{G} = \boldsymbol{\nu}^H \boldsymbol{\Phi}_B$ and $\boldsymbol{h}_{r,e}^H \boldsymbol{\Theta} \boldsymbol{G} = \boldsymbol{\nu}^H \boldsymbol{\Phi}_e$, where $\boldsymbol{\Phi}_B = \mathrm{diag}(\boldsymbol{h}_{r,B}^H)\boldsymbol{G}$ and $\boldsymbol{\Phi}_e = \mathrm{diag}(\boldsymbol{h}_{r,e}^H)\boldsymbol{G}$. Note that the power consumption $P = \boldsymbol{w}\boldsymbol{w}^H$ is derived from the given transmit beamforming vector $\boldsymbol{w}$. Then problem (11) can be reformulated as problem (12) shown at the bottom of this page. Driven by wide applications of the fully-fledged semidefinite relaxation (SDR) technique [12], we tend to apply it to handle $\boldsymbol{\nu}$ and induce problem (13) as below

$$\begin{aligned} \max_{\bar{\boldsymbol{\nu}},\rho} \quad & \rho && (13a)\\ \text{s.t.} \quad & \frac{P\left(\bar{\boldsymbol{\nu}}^H \boldsymbol{R}_B \bar{\boldsymbol{\nu}} + \left\|\boldsymbol{h}_{d,B}^H\right\|^2\right)}{\sigma^2} \ge \rho, && (13b)\\ & \mathbb{E}\left[\frac{P\left(\bar{\boldsymbol{\nu}}^H \boldsymbol{R}_{PE_q} \bar{\boldsymbol{\nu}} + \left\|\boldsymbol{h}_{d,PE_q}^H\right\|^2\right)}{\sigma^2}\right] \le \xi, && (13c)\\ & |\bar{\nu}_n| \le 1, && (13d)\\ & |\bar{\nu}_{N+1}| = 1, && (13e) \end{aligned}$$

where $\boldsymbol{R}_B = \begin{bmatrix} \boldsymbol{\Phi}_B \boldsymbol{\Phi}_B^H & \boldsymbol{\Phi}_B \boldsymbol{h}_{d,B} \\ \boldsymbol{h}_{d,B}^H \boldsymbol{\Phi}_B^H & 0 \end{bmatrix}$, $\boldsymbol{R}_{PE_q} = \begin{bmatrix} \boldsymbol{\Phi}_{PE_q} \boldsymbol{\Phi}_{PE_q}^H & \boldsymbol{\Phi}_{PE_q} \boldsymbol{h}_{d,PE_q} \\ \boldsymbol{h}_{d,PE_q}^H \boldsymbol{\Phi}_{PE_q}^H & 0 \end{bmatrix}$, $\bar{\boldsymbol{\nu}} = \begin{bmatrix} \boldsymbol{\nu} \\ 1 \end{bmatrix}$. Notice that $\bar{\boldsymbol{\nu}}^H \boldsymbol{R}_B \bar{\boldsymbol{\nu}} = \mathrm{Tr}\left(\boldsymbol{R}_B \bar{\boldsymbol{\nu}} \bar{\boldsymbol{\nu}}^H\right)$, $\bar{\boldsymbol{\nu}}^H \boldsymbol{R}_{PE_q} \bar{\boldsymbol{\nu}} = \mathrm{Tr}\left(\boldsymbol{R}_{PE_q} \bar{\boldsymbol{\nu}} \bar{\boldsymbol{\nu}}^H\right)$. Appending $\boldsymbol{V} = \bar{\boldsymbol{\nu}} \bar{\boldsymbol{\nu}}^H$, problem (13) can be reconstructed into

$$\begin{aligned} \max_{\boldsymbol{V},\rho} \quad & \rho && (14a)\\ \text{s.t.} \quad & \mathrm{Tr}\left(\boldsymbol{R}_B \boldsymbol{V}\right) + \left\|\boldsymbol{h}_{d,B}^H\right\|^2 \ge \frac{\sigma^2 \rho}{P}, && (14b)\\ & \mathrm{Tr}\left(\mathbb{E}\left[\boldsymbol{R}_{PE_q}\right] \boldsymbol{V}\right) + \left\|\boldsymbol{h}_{d,PE_q}^H\right\|^2 \le \frac{\sigma^2 \xi}{P}, && (14c)\\ & \boldsymbol{V}_{n,n} \le 1, && (14d)\\ & \boldsymbol{V}_{N+1,N+1} = 1, && (14e)\\ & \boldsymbol{V} \succeq 0, && (14f)\\ & \mathrm{rank}\left(\boldsymbol{V}\right) \le 1. && (14g) \end{aligned}$$

Since the rank-one constraint (14g) is non-convex, we remove it to ensure problem (14) to be solvable, then we can obtain a relaxed version marked as problem (15)

$$\begin{aligned} \max_{\boldsymbol{V},\rho} \quad & \rho && (15a)\\ \text{s.t.} \quad & (14\text{b}), (14\text{c}), (14\text{d}), (14\text{e}), \text{and } (14\text{f}). && (15b) \end{aligned}$$

$$\begin{aligned} \max_{\boldsymbol{\nu},\rho} \quad & \rho && (12a)\\ \text{s.t.} \quad & \frac{P\left(\boldsymbol{\nu}^H \boldsymbol{\Phi}_B \boldsymbol{\Phi}_B^H \boldsymbol{\nu} + \boldsymbol{\nu}^H \boldsymbol{\Phi}_B \boldsymbol{h}_{d,B} + \boldsymbol{h}_{d,B}^H \boldsymbol{\Phi}_B^H \boldsymbol{\nu} + \left\|\boldsymbol{h}_{d,B}^H\right\|^2\right)}{\sigma^2} \ge \rho, && (12b)\\ & \mathbb{E}\left[\frac{P\left(\boldsymbol{\nu}^H \boldsymbol{\Phi}_{PE_q} \boldsymbol{\Phi}_{PE_q}^H \boldsymbol{\nu} + \boldsymbol{\nu}^H \boldsymbol{\Phi}_{PE_q} \boldsymbol{h}_{d,PE_q} + \boldsymbol{h}_{d,PE_q}^H \boldsymbol{\Phi}_{PE_q}^H \boldsymbol{\nu} + \left\|\boldsymbol{h}_{d,PE_q}^H\right\|^2\right)}{\sigma^2}\right] \le \xi, && (12c)\\ & |\nu_n| \le 1. && (12d) \end{aligned}$$

Moreover, the relaxed problem (15) can be equivalently transformed into a feasibility problem

$$\text{find} \quad \boldsymbol{V} \tag{16a}$$

$$\text{s.t.} \quad \mathrm{Tr}\left(\boldsymbol{R}_B\boldsymbol{V}\right) + \left\|\boldsymbol{h}_{d,B}^H\right\|^2 \geq \frac{\sigma^2\rho}{P}, \tag{16b}$$

$$\mathrm{Tr}\left(\mathbb{E}\left[\boldsymbol{R}_{PE_q}\right]\boldsymbol{V}\right) + \left\|\boldsymbol{h}_{d,PE_q}^H\right\|^2 \leq \frac{\sigma^2\xi}{P}, \tag{16c}$$

$$(14\text{d}), (14\text{e}), \text{and } (14\text{f}).$$

Eventually, a convex semi-definite program (SDP) written as problem (16) has been established. Following a bisection search procedure over ρ, we can obtain the optimal solution set $\{\boldsymbol{V}^*, \rho^*\}$ for problem (16).

Now, reconsider problem (14) and pick out suitable $\boldsymbol{V}^*$ from the optimal solution set $\{\boldsymbol{V}^*, \rho^*\}$, where the chosen $\boldsymbol{V}^*$ satisfies constraint (14g). However, for those who comply with $\mathrm{rank}\left(\boldsymbol{V}^*\right) > 1$, we apply Guassian randomization procedure [12] to generate high-quality rank-one $\boldsymbol{V}^*$. Ultimately, the optimal $\boldsymbol{\nu}^*$ can be extracted from the treated $\boldsymbol{V}^*$.

B. Transmit Beamforming Weight Vector Optimization

For a certain reflective beamforming vector $\boldsymbol{\nu}^*$, we next optimize the transmit beamforming vector $\boldsymbol{w}$. We define a beamforming weight vector $\boldsymbol{a} \in \mathbb{R}^M$ to restrict $\boldsymbol{w}$ to lie in the null space of the AEves' channel matrix $\left[\boldsymbol{h}_{AE_1}, \boldsymbol{h}_{AE_2}, \ldots, \boldsymbol{h}_{AE_{N_A}}\right]^H$, and design the beamforming vector $\boldsymbol{w}$ in the commensurate manner of (7)

$$\boldsymbol{w} = \boldsymbol{\varphi}_{AE}\boldsymbol{\varphi}_{AE}^H\boldsymbol{a}, \tag{17}$$

where $\boldsymbol{\varphi}_{AE} \in \mathbb{C}^{M\times(M-N_A)}$ is a matrix, and the null space of AEves' effective channel matrix can be constituted by a basis comprised of its $M - N_A$ columns. This design ensures the SNR of AEves to be minimized. Let $\boldsymbol{\Psi} = \boldsymbol{\varphi}_{AE}\boldsymbol{\varphi}_{AE}^H$, i.e., $\boldsymbol{w} = \boldsymbol{\Psi}\boldsymbol{a}$, then problem (10) has numerically evolved as a function of transmit beamforming weight vector $\boldsymbol{a}$ as follows

$$\max_{\boldsymbol{a}} \quad \frac{\boldsymbol{a}^H\mathbf{H}_B^{\boldsymbol{\Psi}}\boldsymbol{a}}{\sigma^2} \tag{18a}$$

$$\text{s.t.} \quad \frac{\boldsymbol{a}^H\overline{\mathbf{H}}_{PE}^{\boldsymbol{\Psi}}\boldsymbol{a}}{\sigma^2} \leq \xi, \tag{18b}$$

$$\|\boldsymbol{\Psi}\boldsymbol{a}\|^2 \leq P_A, \tag{18c}$$

where $\mathbf{H}_B^{\boldsymbol{\Psi}} = \boldsymbol{\Psi}^H\boldsymbol{h}_B^H\boldsymbol{h}_B\boldsymbol{\Psi}$, and $\overline{\mathbf{H}}_{PE}^{\boldsymbol{\Psi}} = \boldsymbol{\Psi}^H\overline{\mathbf{H}}_{PE}\boldsymbol{\Psi}$.

To manage the non-convexity of problem (18), the successive convex approximation (SCA) technique can precisely transform the optimization goal (18a) into an affine form. Notice that the first-order Taylor approximation is the lower bound of a convex function at any given point. Thus, with a given point $\boldsymbol{a}_i$, we have

$$\begin{aligned}&\frac{\boldsymbol{a}^H\mathbf{H}_B^{\boldsymbol{\Psi}}\boldsymbol{a}}{\sigma^2}\\ &\geq \frac{\boldsymbol{a}_i^H\mathbf{H}_B^{\boldsymbol{\Psi}}\boldsymbol{a}_i}{\sigma^2} + \frac{2}{\sigma^2}\left(\mathbf{H}_B^{\boldsymbol{\Psi}}\,\boldsymbol{a}_i\right)^H(\boldsymbol{a}-\boldsymbol{a}_i)\\ &\triangleq g\left(\boldsymbol{a};\boldsymbol{a}_i\right).\end{aligned} \tag{19}$$

Algorithm 1 CCP-based solution to problem (18).

given an initial feasible point $\boldsymbol{a}_0$

$i := 0$

repeat

1. *Convexify*. Form
$$g\left(\boldsymbol{a};\boldsymbol{a}_i\right) = \frac{\boldsymbol{a}_i^H\mathbf{H}_B^{\boldsymbol{\Psi}}\boldsymbol{a}_i}{\sigma^2} + \frac{2}{\sigma^2}\left(\mathbf{H}_B^{\boldsymbol{\Psi}}\,\boldsymbol{a}_i\right)^H(\boldsymbol{a}-\boldsymbol{a}_i)$$
2. *Solve*. Set the value of $\boldsymbol{a}_{i+1}$ to a solution of the convex problem
$$\begin{aligned}\max_{\boldsymbol{a}} \;& g\left(\boldsymbol{a};\boldsymbol{a}_i\right)\\ \text{s.t.} \;& \frac{\boldsymbol{a}^H\overline{\mathbf{H}}_{PE}^{\boldsymbol{\Psi}}\boldsymbol{a}}{\sigma^2} \leq \xi,\\ & \|\boldsymbol{\Psi}\boldsymbol{a}\|^2 \leq P_A.\end{aligned}$$
3. *Update iteration*. $i := i + 1$.

until $g\left(\boldsymbol{a};\boldsymbol{a}_{i+1}\right) - g\left(\boldsymbol{a};\boldsymbol{a}_i\right) \leq \epsilon$.

TABLE I
SIMULATION PARAMETERS

Parameter	Value
Path loss at 1 m	$L_0 = -30$ dB
Path loss exponent	$\alpha_{ab} = \alpha_{ae} = 3.4, \alpha_{ar} = 2.0,$ $\alpha_{rb} = \alpha_{re} = 2.2.$
Rician factor	$\kappa_{ab} = \kappa_{ae} = 0, \kappa_{ar} = 10,\ \kappa_{rb} = \kappa_{re} = 10.$
Other parameters	$\sigma^2 = -86$ dBW, $\epsilon = 10^{-3},\ P_A =$ 14 dBW, $\xi = 15$ dB.

Then we introduce convex-concave procedure (CCP) summarized in Algorithm 1 above to solve the aforementioned problem (18).

Remarks:

- Given that CCP is a heuristic program, a nontrivial feasible initial point (FIP) is essential to the quality of the solution.
- Note that our proposed algorithm abides by the CCP framework and hence a FIP guarantees the algorithm convergence to a stationary point [13].

In this way, for $i = 0, 1, 2, \ldots$ until convergence, we finally obtain the optimal $\boldsymbol{a}^*$ and $\boldsymbol{w}^*$.

IV. SIMULATION RESULT

In this section, we aim to present numerical results based on the simulation parameters set in Table I [8]. Consistent with the 3D deployment mentioned in [14], Alice, Rose and Bob are located at (5, 0, 10), (2, 58, 0) and (0, 60, 10). We consider the case where all interceptors are randomly distributed within a circle centered on Bob. As the system is set in a high-density urban scenario, Rose is assumed to be placed on the surface of a building. Meanwhile, the Eves and Bob are located on the ground. $\boldsymbol{h}_{ab}^H = \sqrt{L_0 d_{ab}^{-\alpha_{ab}}}\boldsymbol{g}_{ab}$ generates the downlink channel response from Alice to Bob, where the distance between Alice and Bob is denoted by d_{ab}, and the small-scale fading component $\boldsymbol{g}_{ab}$ is defined as Rician fading and given by $\boldsymbol{g}_{ab} = \sqrt{\kappa_{ab}/(1+\kappa_{ab})}\boldsymbol{g}_{ab}^{\mathrm{LoS}} + \sqrt{1/(1+\kappa_{ab})}\boldsymbol{g}_{ab}^{\mathrm{NLoS}}$. κ_{ab} is the Rician

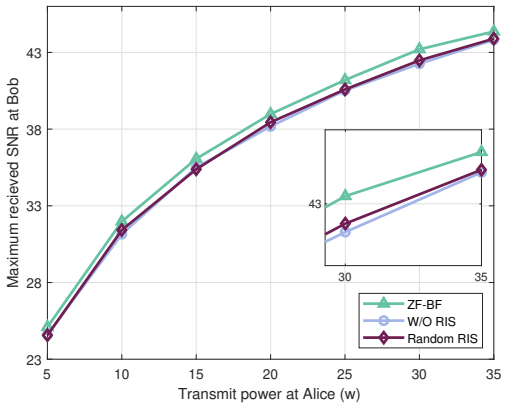

Fig. 2. The SNR at Bob versus transmit power at Alice.

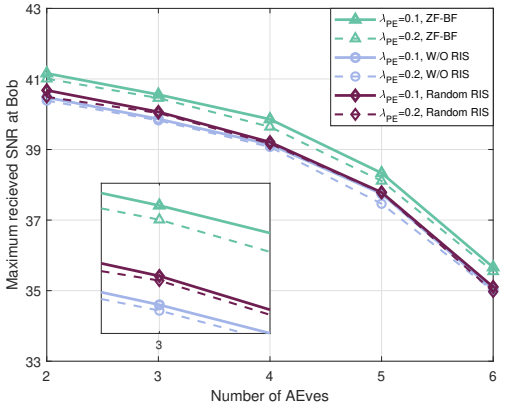

Fig. 3. The SNR at Bob versus the number of AEves.

factor, while $\boldsymbol{g}_{ab}^{\mathrm{LoS}}$ and $\boldsymbol{g}_{ab}^{\mathrm{NLoS}}$ are the deterministic line-of-sight and Rayleigh fading component, respectively. Such channel model is employed for all others. Unlike receivers on the ground, Rose is deployed on a higher place, which creates less scattering propagating environment from Alice to Rose, thus it is rational to set pathloss component $\alpha_{ar} < \alpha_{ak}, k \in \{b, e\}$ [15]. Additionally, zero-forcing without RIS (denoted as "W/O RIS") and random phases at RIS (denoted as "Random RIS") are introduced as benchmark schemes.

As shown in Fig. 2, the maximum received SNR at Bob is on a steady rise as transmit power budget continues to increase. Our speculation for such flattening curves is that when P_A is sufficiently large, transmit power budget cannot be fully utilized, otherwise it is unable to constrain the PEve's SNR under a specified threshold. On the whole, our proposed design (denoted as "ZF-BF") outperforms the benchmarks. The "W/O RIS" scheme is not asymptotically optimal since the RIS-assisted scheme can mitigate the co-channel interference by optimizing the reflective beamformer.

Fig. 3 demonstrates the SNR for different densities of PEves λ_{PE} when variable numbers of AEves are arbitrarily situated within a circle of radius 1.5 m. The proposed secure beamforming design yields a higher SNR performance than the benchmarks. Also, as the number of AEves increases, the received SNR at Bob decreases. This is because the rank of AEve's null space matrix decreases when the number of AEves grows, leading to limited optimal beamforming vectors and a declining achievable SNR. Moreover, higher density of PEves indicates more PEves get involved, which increases the likelihood of information divulgence at Bob.

V. Conclusion

In this correspondence, we proposed an innovative zero-forcing beamforming scheme against active and passive eavesdroppers in a RIS-enhanced secure transmission system. Since the acquisition of the CSI for PEves is difficult, we utilize stochastic geometry to model the PEves' locations. The reflective beamforming vector and the transmit beamforming vector have been alternatively optimized by applying the SDR technique and monotonically converging CCP algorithm, respectively. Given the fact that both AEves and PEves may be present in reality, it can be concluded that the secure beamforming design provides practical engineering guidelines for RIS-aided transmission systems in urban scenarios.

References

[1] K. Feng, X. Li, Y. Han, S. Jin and Y. Chen,"Physical Layer Security Enhancement Exploiting Intelligent Reflecting Surface,"in *IEEE Communications Letters*, vol. 25, no. 3, pp. 734-738, March 2021.

[2] A. Yener and S. Ulukus, "Wireless Physical-Layer Security: Lessons Learned From Information Theory," in *Proceedings of the IEEE*, vol. 103, no. 10, pp. 1814-1825, Oct. 2015.

[3] J. Li, A. P. Petropulu, and S. Weber, "On cooperative relaying schemes for wireless physical layer security " *IEEE Trans. Signal Process.*, vol. 59, no. 10, pp. 4985–4997, Oct. 2011.

[4] Y. Sun, D. W. K. Ng, J. Zhu, and R. Schober, "Robust and secure resource allocation for full-duplex MISO multicarrier NOMA systems," *IEEE Trans. Commun.*, vol. 66, no. 9, pp. 4119–4137, Sep. 2018.

[5] L. Dong, Z. Han, A. P. Petropulu, and H. V. Poor, "Improving wireless physical layer security via cooperating relays,"*IEEE Trans. Signal Process.*, vol. 58, no. 3, pp. 1875–1888, Mar. 2010.

[6] Q. Wu and R. Zhang, "Towards Smart and Reconfigurable Environment: Intelligent Reflecting Surface Aided Wireless Network," in *IEEE Communications Magazine*, vol. 58, no. 1, pp. 106-112, January 2020.

[7] A. Makarfi, K. Rabie, O. Kaiwartya, O. Badarneh, G. Nauryzbayev, and R. Kharel, "Physical layer security in RIS-assisted networks in Fisher–Snedecor composite fading," in *Proc. 12th Int. Symp. Commun. Syst., Netw. Digit. Signal Process. (CSNDSP)*, Jul. 2020, pp. 1–6.

[8] H. Shen, W. Xu, S. Gong, Z. He, and C. Zhao, "Secrecy rate maximization for intelligent reflecting surface assisted multi-antenna communications," *IEEE Commun. Lett.*, vol. 23, no. 9, pp. 1488–1492, Sep. 2019.

[9] K. Feng, X. Li, Y. Han, S. Jin, and Y. Chen, "Physical layer security enhancement exploiting intelligent reflecting surface," *IEEE Commun. Lett.*, vol. 25, no. 3, pp. 734–738, Mar. 2021.

[10] S. Hong, C. Pan, H. Ren, K. Wang and A. Nallanathan,"Artificial-Noise-Aided Secure MIMO Wireless Communications via Intelligent Reflecting Surface," in *IEEE Transactions on Communications*, vol. 68, no. 12, pp. 7851-7866, Dec. 2020.

[11] X. Guan, Q. Wu, and R. Zhang, "Intelligent reflecting surface assisted secrecy communication: Is artificial noise helpful or not?" *IEEE Wireless Commun. Lett.*, vol. 9, no. 6, pp. 778–782, Jun. 2020.

[12] Z.-Q. Luo, W.-K. Ma, A. M.-C. So, Y. Ye and S. Zhang, "Semidefinite relaxation of quadratic optimization problems", *IEEE Signal Process. Mag.*, vol. 27, no. 3, pp. 20-34, May 2010.

[13] G. R. Lanckriet and B. K. Sriperumbudur, "On the convergence of the concave-convex procedure", *Proc. Adv. Neural Inf. Process. Syst.*, pp. 1759-1767, 2009.

[14] S. Wang and Q. Li, "Distributionally Robust Secure Multicast Beamforming With Intelligent Reflecting Surface," in *IEEE Transactions on Information Forensics and Security*, vol. 16, pp. 5429-5441, 2021.

[15] Z. Ji et al., "Secret key generation for intelligent reflecting surface assisted wireless communication networks", *IEEE Trans. Veh. Technol.*, vol. 70, no. 1, pp. 1030-1034, Jan. 2021.